NAL PROPOSAL No. 134

Scientific Spokesman:
V. P. Kenney
Physics Department
University of Notre Dame
Notre Dame, Indiana 46556

Telephone: 219 - 283-7451

STUDY OF MULTIPION PRODUCTION IN HIGH ENERGY $\pi^- p$ INTERACTIONS AT NAL

N. N. Biswas, N. M. Cason, V. P. Kenney
W. D. Shephard and D. W. Thomas
plus graduate students

University of Notre Dame

April 26, 1971

I. COVER PAGE

Title: STUDY OF MULTIPION PRODUCTION IN HIGH ENERGY $\pi^- p$ INTERACTIONS AT NAL.

Abstract: We propose to study the inclusive reactions $\pi^- + p \rightarrow \pi^- +$ anything in the 30-in. hydrogen bubble chamber at 50, 150, and 300 GeV/c. The majority of the data will be taken at 150 GeV/c to optimize the physics obtainable in the "bare" configuration of the 30-in. chamber. The data at 50 and 300 GeV/c will serve to test scaling behavior and to relate our results to those obtained at lower-energy accelerators. We will measure distributions of the scaling variable x and the transverse momentum Q as functions of each other and of the charge-multiplicity n. These and related distributions will be compared with the predictions of multiperipheral, limiting fragmentation, parton, quark, thermodynamic and other models for hadron interactions at high energies. This experiment will extend Notre Dame measurements at "conventional" accelerator energies (8 and 18 GeV/c) to energies where asymptotic approximations may be valid and some discrimination among the models should be possible. From our own experience it is clear that the 30-in. chamber in its "bare" configuration can yield significant results within 10 weeks from data acquisition.

Names of Experimenters: N. N. Biswas, N. M. Cason, V. P. Kenney, W. D. Shephard, and D. W. Thomas, plus graduate students.

Affiliation: University of Notre Dame, Notre Dame, Indiana 46556

Date: April 26, 1971

Spokesman: V. P. Kenney, Physics Department, University of Notre Dame, Notre Dame, Indiana 46556, Telephone: 219-283-7451

TABLE OF CONTENTS PAGE

I. Cover Page -- Title and Abstract 1

II. Summary 3

III. Physics Justification 5

A. Introduction

B. Scaling and Factorization: Multiperipheral and Fragmentation Models 8

C. Distributions of Q and Q^2: Thermodynamic and Resonance Models 13

D. Charged-Particle Multiplicities 15

E. Topological Cross Sections 17

IV. Experimental Arrangement and Analysis 18

A. Beam 18

B. Upstream Instrumentation 19

C. Picture Requirements 20

D. Data Analysis 21

E. Resolution 22

References 26

Figure Captions 29

II. SUMMARY

We are proposing a study at NAL of the inclusive reactions $\pi^- + p \rightarrow \pi^-$ + anything at incident momenta of 50, 150 and 300 GeV/c in the "bare" 30-in. hydrogen bubble chamber without additional downstream hardware. We suggest the desirability of performing this experiment at the earliest possible date that the chamber and beam are available. The experiment can yield significant results on inclusive reactions within 10 weeks after acquisition of data and can provide information needed in the design of later experiments involving hybrid configurations of bubble chamber and downstream spectrometer. Notre Dame proposes to provide hardware and software for putting information from proportional chambers and Cerenkov counters in the beam-line onto magnetic tape.

In Section III we describe the physics which can result from this experiment. By extrapolation from the results we have already obtained at lower energies we show that by analysis of distributions of the scaling variable x for longitudinal momentum, the transverse momentum Q, and the charge multiplicity n: (a) quantitative tests of scaling behavior may be made in systematic fashion over a wide range of s; (b) factorization can be tested up to $s = 564$ GeV^2; (c) a distinction between multiperipheral and limiting fragmentation models may be made on the basis of $d\sigma/dx$ at $x = 0$; (d) a clear test can be made of the Yen-Berger hypothesis that peaks observed at low Q^2 for small $|x|$ are due to peripherally-produced resonances; (e) apparent agreement of Q-distributions with simple predictions of thermodynamic models can be checked; (f) a measurement of track multiplicities should allow a decision between models predicting a ln s dependence of

$< n >$ and those predicting an s^{α} dependence; (g) topological cross sections can be measured for all multiplicities. Several of these tests are currently only practical in bubble chambers; for most of them a bubble-chamber experiment is the best way to obtain early results.

In Section IV we show that the requirements for beam and accelerator time at NAL are modest and thus the experiment should be possible at an early date within the framework of current NAL planning. In Section IV. B the desirability of additional instrumentation of the beam is discussed. Although this additional instrumentation is not essential for the experiment proposed here, it will be necessary for effective future utilization of the bubble chamber facility.

In Section IV. D we demonstrate the capability of Notre Dame to obtain results rapidly and effectively in an "inclusive" experiment of the type proposed. Finally we provide evidence that the resolution obtainable in the 30-in. chamber is adequate to provide the information needed for the proposed physics.

III. PHYSICS JUSTIFICATION

A. Introduction.

The study of the characteristics of inelastic processes in hadron-hadron collisions is of considerable interest. At high energies the inelastic processes are dominant, the production of resonances in any specific channel becomes relatively small, and many particles are involved. It is of particular interest[1-5] to study processes such as

$$A + B \rightarrow C + \text{anything}$$

which are, in the terminology of Feynman, "inclusive processes" with no constraints on the final-state products other than the presence of C, the particle being studied. The cross sections for such processes are expected to remain significant as the incident momentum is increased.

Investigations have already been carried out at conventional accelerator energies (below 30 GeV) on the reactions:

$$\pi^{\pm}p \rightarrow \pi^{-} + \text{anything}^{6,7}, \tag{1}$$

$$K^{+}p \rightarrow \pi^{-} + \text{anything}^{8}, \tag{2}$$

$$pp \rightarrow \pi^{-} + \text{anything}^{9}. \tag{3}$$

For example, the Notre Dame group[6] has recently studied $\pi^{\pm}p$ interactions at 8 and 18.5 GeV/c. The results we have obtained are typical of the situation at current accelerator energies. It is expected that results from Serpukhov will soon be available at somewhat higher energies (up to 70 GeV). Further progress will require the results of experiments at NAL such as the experiment proposed here.

Various models of high energy hadron-hadron interactions have been proposed including the parton model[1], the limiting-fragmentation model[2], quark models[7], multiperipheral models[4], thermodynamic models[3] and others[5]. Predictions are made about the distributions of the scaling variable x and the transverse momentum Q. The scaling variable x is defined as $x \equiv p_{\parallel}/p_o$ where $p_{\parallel}$ is the longitudinal momentum of a secondary particle in the overall center-of-mass (c.m.) system and p_o is the c.m. momentum of the incident pion.[10] Data obtained at presently available energies[6-9] reveal some general features of multiparticle interactions that are also observed at cosmic ray energies and which must be explained by any successful model. These include: (a) small transverse momenta ($< Q > \sim .3-.5$ GeV/c); (b) relatively low multiplicity ($< n > \sim \ln s$ or $s^{1/4}$); (c) longitudinal momenta $< p_{\parallel} >$ much greater than $< Q >$ at high energies. However, data at NAL energies are needed to distinguish clearly among the models and to establish or disprove predictions such as scaling and factorization.

In order to obtain this information at the earliest possible date, it seems desirable to design and to perform experiments of the minimum complexity necessary to obtain significant results. We believe that access to significant physics may be obtained via analysis of unconstrained events observed in the 30-in. hydrogen bubble chamber in its initial "bare" configuration using the π^- beam at NAL. Such experiments, in addition to providing information needed for the effective execution of second-generation hybrid spectrometer experiments, promise to provide information which should

independently be sufficient to settle many points about high-energy interactions. Our proposal is based on our current studies of reaction (1) at 8 and 18.5 GeV/c and on our studies of what can be measured in the "bare" 30-in. bubble chamber.

The experiment requires a 200,000 picture exposure at 150 GeV/c incident π^- momentum with an average of 10 tracks/picture, and exposures of 100,000 pictures each at incident π^- momenta of 50 and 300 GeV/c. The principal momentum of 150 GeV/c is chosen so that good measurements on x can be made out to $x \approx +0.1$ at as high an incident momentum as possible. The 50 GeV/c portion of the experiment will allow a direct connection with results at lower energy. The 300 GeV/c exposure will extend information on energy dependence toward "asymptopia" with statistics sufficient to check scaling over a wide range from $s = 16\ \mathrm{GeV}^2$ to $s = 564\ \mathrm{GeV}^2$. (See Table I which includes the energies of our previous experiments together with the proposed energies.)

TABLE I

Comparison of Incident Momenta and Energies

p_{in} (GeV/c)	$\sqrt{s}$ (GeV)	s (GeV^2)	p_o (GeV/c)	ln s
8.0	4.0	16.0	1.88	2.77
18.5	6.0	35.6	2.91	3.57
50.0	9.7	94.7	4.82	4.55
150.0	16.8	282.2	8.37	5.65
300.0	23.7	563.6	11.85	6.34

We now consider some specific features of inclusive reactions which we expect to study in the proposed experiment and relate them to currently available results and to the predictions of models.

B. Scaling and Factorization: Multiperipheral and Fragmentation Models

The scaling property of momentum distributions, first proposed by Feynman[1], has been found to hold for a variety of models[11-13]. The conjecture is that

$$\frac{2E}{\pi\sqrt{s}} \frac{d^2\sigma}{dx dQ^2} = f(x, Q, s) \xrightarrow[s \to \infty]{} f(x, Q)$$

Details vary in the different models[11], but the apparently fundamental nature of the scaling hypothesis makes tests of its validity imperative.

A further hypothesis, that of "factorization", suggests that $f(x, Q)$ can be factorized into independent functions of x and Q for large s. Data at present available energies suggest that, while there appears to be evidence for some form of scaling behavior, there is as yet no quantitative support for factorization. The Notre Dame data for $\pi^{\pm} p \to \pi^{-}$ + anything at 8 and 18.5 GeV/c have been studied to determine the dependence of the cross section on x and Q. Representative x-distributions are shown in Fig. 1 and Q^2 distributions are shown in Fig. 2. The x-distributions exhibit dependence on Q and on the prong number n; the Q-distributions depend on x and n. To illustrate this dependence, the data have been fitted to expressions of the form

$$dN/dQ = CQ^{3/2} \exp\left[-aQ\right]$$

and

$$dN/dx = C \exp\left[-b|x|\right] .$$

The coefficient a has been determined as a function of n and x and the coefficient b as a function of n and Q^2 as shown in Fig. 3. The dependence of a on x and of b on Q^2, shown in Figs. 3b, d, f and h, indicates that $d^2\sigma/dxdQ^2$ cannot be factorized into independent functions of x and Q^2. We also find that $(d^2\sigma/dxdQ^2)E$ cannot be factorized into independent functions of x and Q^2. Results consistent with ours have been found for K^+p interactions[8] at 11.8 GeV/c. Since factorization is predicted to hold in the asymptotic limit, high-energy experiments are clearly required.

Values of b are found to differ for $x > 0$ and $x < 0$ in both the π^+p (no "leading particle" contribution) and π^-p cases[6]. The same is true for K^+p data[8]. For $x < 0$, our values of b for π^+p and π^-p are similar, and are in qualitative agreement with values for π^-p data at 8 and 25 GeV/c and with K^+p and pp data[10] as shown in Table II. For $x < 0$, the values of a are also similar for $\pi^\pm p$ and pp interactions as shown in Table III. (We find that da/dn and db/dn, the slopes of the straight lines in Figs. 3a, c, e, and g, are also in agreement with results for pp interactions.) This suggests that fragmentation of the proton is independent of the projectile particle $\pi^\pm$, K^+, or p. The variation of target fragmentation with energy can thus be tested in the proposed experiment.

The equality of the values of b for $x < 0$ in different reactions might suggest scaling of $d\sigma/dx$; this would conflict with the Feynman hypothesis of scaling in $(2E/\pi\sqrt{s})\ (d^2\sigma/dxdQ^2)$. However, when we

Table II

Fits to $dN/dx = C \exp\left[-b|x|\right]$ for $x < 0$.

Reaction	$\sqrt{s}$	Number n of charged particles					
		All Prongs	2	4	6	8	10
$\pi^- p$	4.0	-	7.71 ± 0.24	7.60 ± 0.09	10.24 ± 0.19	11.17 ± 0.55	-
$K^+ p$	4.8	10.6 ± 0.7	-	-	-	-	-
$\pi^+ p$	6.0	10.29 ± 0.07	-	8.36 ± 0.10	10.89 ± 0.12	13.02 ± 0.23	14.24 ± 0.60
$\pi^- p$	6.0	9.83 ± 0.08	8.82 ± 0.34	8.44 ± 0.10	10.32 ± 0.14	12.44 ± 0.26	14.30 ± 0.79
$\pi^- p$	7.0	-	-	8.38 ± 0.62	10.43 ± 0.20	12.70 ± 0.27	15.34 ± 0.46
pp	6.0	-	-	7.29 ± 0.10	10.08 ± 0.20	12.80 ± 0.34	-

Table III

Values of a in the expression $dN/dQ = CQ^{3/2} \exp\left[-aQ\right]$

Number of charged prongs		a $(GeV/c)^{-1}$		
		$\pi^- p$	$\pi^+ p$	pp[a)]
All	x > 0	6.75 ± 0.02	7.67 ± 0.03	
	x < 0	7.86 ± 0.04	8.05 ± 0.05	
2	x > 0	5.88 ± 0.05		
	x < 0	7.88 ± 0.18		
4	x > 0	6.61 ± 0.04	7.12 ± 0.04	7.77 ± 0.09
	x < 0	7.49 ± 0.06	7.65 ± 0.06	
6	x > 0	7.10 ± 0.05	7.68 ± 0.04	8.10 ± 0.11
	x < 0	7.86 ± 0.06	8.05 ± 0.05	
8	x > 0	7.74 ± 0.08	8.47 ± 0.08	8.85 ± 0.15
	x < 0	8.45 ± 0.12	8.50 ± 0.09	
10	x > 0	8.80 ± 0.27	9.66 ± 0.20	
	x < 0	10.24 ± 0.29	10.56 ± 0.22	

compare the distributions for $(d\sigma/dxdQ^2)$ at 8 and 18.5 GeV/c with the distributions of $(2E/\pi\sqrt{s})$ $(d^2\sigma/dxdQ^2)$ at the same two energies (See Fig. 4) we find that the former distributions differ more, both in absolute value near $x = 0$ and in shape than do the latter. This suggests that Feynman's hypothesis is more nearly correct even at the low energies now available. We do, however, still observe some difference in absolute magnitude for $f(x, Q, s)$ at 8 and 18.5 GeV/c. The corresponding distributions for π^- from π^+p at 18.5 GeV/c differ by a much greater amount. Thus it is important to test scaling over the wider range of energies of the proposed experiment to see if a limiting distribution is approached at higher s and to see if the differences for different incident particles are diminished.

The possibility of examining $(d^2\sigma/dxdQ^2)$ near $x = 0$ in the proposed experiment is of special interest. It may be possible to distinguish between various models[13] such as the multiperipheral models and the limiting fragmentation model. The predictions of the models vary for $(d\sigma/dx)$ near $x = 0$. Feynman has suggested that for $s \to \infty$, the x-distribution will be flat in the region of "wee" x. $\left(|x| \lesssim \frac{1\ \mathrm{GeV/c}}{p_o}\right)$. In contrast, the limiting fragmentation model without "pionization" would seem to predict a dip at $x = 0$ as $s \to \infty$. Distributions of variables such as the "rapidity" or "boost" variables suggested by Feynman[1] and DeTar[11] may be of special value here since the region near $x = 0$ is spread out. If the multiperipheral models are valid, distributions of the rapidity variable $w = -\ln\left(\frac{E-p_{\parallel}}{\sqrt{Q^2 + m^2}}\right)$ are

expected to exhibit a plateau at high incident energies. In contrast, the limiting fragmentation models would suggest a "two-peaked" distribution although "pionization" might modify this. At 18.5 GeV/c, rapidity distributions show a tendency to flatten near $w = 0$ (see Fig. 5) but this is not yet pronounced. In the proposed experiment we will examine a wider range of w. In addition to all values of w corresponding to $x < 0$ we can examine the full range of w corresponding to Feynman's "wee" x region. The shapes of the rapidity distributions and their variation with incident energy will provide significant tests of the various models.

C. Distributions of Q and Q^2: Thermodynamic and Resonance Models.

Distributions of the transverse momentum exhibit dependence on the multiplicity n and on x as illustrated in Fig. 2 which shows typical Q^2 distributions for 18.5 GeV/c π^+p interactions. Data for π^-p interactions exhibit similar features. An interesting feature of the distributions is the steep slopes at small Q^2 seen for all values of n when $|x|$ is small. The slopes at low Q^2 become less steep for larger $|x|$. The origin of these low-Q^2 peaks is not yet clearly established. Yen and Berger[14] have suggested that they are evidence for the importance of resonances in high-multiplicity events. The peripheral production and fore-aft decay of low-mass resonances could conceivably produce the observed low-Q^2 peaks. Such resonances should be more important for low-multiplicity final states and should be predominantly of the same charge as the initial particles. Thus peaks in π^- distributions

should be less prominent for π^+p than for π^-p interactions if meson resonances were responsible. However, at 18.5 GeV/c we observe peaks of approximately equal prominence for π^+p and π^-p interactions. If peripherally-produced low-mass baryon resonances are responsible, the effects might be the same in π^+p and π^-p data. A better test for the importance of resonances can be made by looking for similar effects in π^- distributions at the higher incident momenta of the proposed experiment. It is kinematically possible at 18.5 GeV/c for π^- from peripherally-produced low-Mass N^{*+} decaying to $p\pi^+\pi^-$ to appear at x-values consistent with the observed low-Q^2 peaks. At higher incident energies, calculations based on the kinematics of such decays suggest that contributions from such a source will be greatly reduced and will be limited to smaller values of x.

If the features of the transverse momentum distributions are not explained by resonance production, they must somehow be explained by other means. The predictions of available models as to the detailed shapes expected for the Q-distributions are limited. Models such as the usual multiperipheral model predict the dominance of small Q at all x, but generally do not predict detailed shapes. Thermodynamic models[3], however, do provide predictions for Q-distributions, even though their validity seems limited to an average over all multiplicities. The models predict x-dependent Q-distributions, but require additional elaboration before they can predict the details of this x-dependence. In view of their ability to make predictions unavailable from other sources, a test of these

predictions at high energies is of value.

In Fig. 6 are shown representative Q-distributions at 18.5 GeV/c for several ranges of x. These distributions show a shift in the position of the peak towards higher Q and a broadening of the peak with increasing $|x|$. These features correspond to the increase in slope of the Q^2 distributions at low Q^2 observed for increasing $|x|$ in Fig. 2b. We have tried fitting these distributions in terms of the thermodynamic model. The Q-distribution predicted by the simplest form of Hagedorn's thermodynamic model is

$$dN/dQ = kQ \left[\exp (E/T) - 1\right]^{-1} dx, \qquad (4)$$

where

$$E = \left[Q^2 + (xp_o)^2 + m_\pi^{\ 2}\right]^{1/2} .$$

The smooth curves in Fig. 6 show fits obtained by numerical integration over a range of x. We find that at 18.5 GeV/c the x-dependence of these Q-distributions for all n is described well by expression (4) with T = 118 MeV. For K^+p interactions at 11.8 GeV/c, Lander[8] finds similar agreement with $T \approx 120$ MeV. The model predicts that the parameter T should approach 160 MeV in the high-energy limit. To test this prediction and to determine whether the apparent agreement at low energy is significant we need to extend the measurements to higher incident momenta. In the proposed experiment we will be able to study dN/dQ for a wide range of x at all the proposed momenta.

D. Charged-Particle Multiplicities.

The distributions of charged-particle multiplicities and the values of mean multiplicity as a function of energy as determined in the proposed

experiments are of considerable interest. There are various predictions[5] of the models which may be tested. Several models -- multiperipheral, thermodynamic, etc. -- predict Poisson or approximately-Poisson distributions for the number of pions or of pion pairs. These predictions are in qualitative agreement with experiments at currently available energies and with the limited cosmic-ray data available. There are differences in the predictions of the models for the variation of $< n >$ with s. For example, the multiperipheral models predict a ln s dependence for $< n >$ while the thermodynamic models predict a power law, s^{α} where α may be $\sim 1/4$. Experiments at incident energies up to 30 GeV have been unable to distinguish among these possibilities. With the wider range of s available in the proposed experiment combined with current data at lower energies a decision should be possible. In Table IV are shown the values expected for $< n_- >$, the average number of negative tracks, calculated from data at 8 and 18.5 GeV/c π^- data with different assumptions for the s dependence.

Table IV

Average π^- Multiplicity as a Function of Incident Momentum

p_{in} (GeV/c)	ln s	$< n_- >^a$	$s^{1/4}$	$< n_- >^b$
8.0	2.77	1.65[c]	2.00	1.69
18.5	3.57	2.11[c]	2.44	2.06
50.0	4.55	2.67	3.12	2.64
150.0	5.65	3.31	4.10	3.46
300.0	6.34	3.70	4.87	4.11

a) Calculated from $< n_- > = .575 \ln s + .057$
b) Calculated from $< n_- > = .845\ s^{1/4}$
c) Experimental values

We will study not only the mean multiplicity as a function of energy, but also the distribution of multiplicity.

E. Topological Cross Sections.

As a by-product of the studies proposed for this experiment, it will be possible to determine topological cross sections even for high-multiplicity topologies, to an accuracy of a few per cent. Accuracy will be reduced for two-prong and zero-prong events because of the usual problems of scanning bias against low-multiplicity events and small-angle scatterings. The only additional effort necessary will be careful beam count. This will be necessary in any case so that we can compare results at different incident energies in the tests of the scaling hypothesis.

IV. EXPERIMENTAL ARRANGEMENT AND ANALYSIS

A. Beam.

The beam described by Lach and Pruss[15] designed to service the 30-in. chamber will be completely adequate for this experiment. Negative pions at 50, 150, and 300 GeV/c are produced and reach the chamber in sufficient number with very modest intensity requirements on the proton flux. For example, the Hagedorn-Ranft model indicates that $< 1.5 \times 10^7$ interacting protons of 500 GeV/c would be sufficient to provide 10 π^- at the bubble chamber with $\Delta p/p = 0.1\%$ for any of our proposed incident momenta. Since we plan to use unconstrained events the momentum spread in the beam is small enough to pose no problem. The proposed divergence of the beam at the chamber is comparable to the angular resolution obtainable for secondary tracks in the 30-in. bubble chamber and thus should create no problem. It should be possible to map the direction of beam particles as a function of their position when entering the chamber to reduce further the uncertainties due to beam direction. The proposed maximum vertical size of the beam would be desirable in order to spread the beam tracks as much as possible for easy scanning and measurement. A fast kicker magnet in the beam would be useful, but not essential for this "bare chamber" experiment.

The time required to obtain the pictures will depend on whether multipulsing of the 30-in. bubble chamber is possible with the available beam. The chamber has previously operated in a multipulsing

mode and has provided pictures of high quality adequate for our purposes. We suggest beam operation to allow multipulsing of the chamber if it is feasible.

Since the beam is unseparated, a contamination of K^-'s and $\bar{p}$'s will be present. Estimates of this contamination range from ~ 1% to ~ 20%[16]. (The μ^- contamination due to π decay in the beam will range from 0.34% at 50 GeV to 0.05% at 300 GeV, assuming those μ's with $\Delta p/p_{beam} > .5\%$ will not traverse the beam and can be safely ignored.)

B. Upstream Instrumentation.

Further instrumentation of the beam, including Cerenkov counters for particle identification and proportional chambers for determining the position and momentum of each beam particle, will be certainly useful, but not essential for this experiment. Instrumentation upstream will be essential for second-generation hybrid experiments, if a downstream momentum spectrometer is to be used to best advantage. Notre Dame

proposes to provide instrumentation to interface a small computer to the output of the proportional chambers and Cerenkov counter planned for beam instrumentation and to provide hardware and software as necessary for magnetic tape output of the upstream beam information. We believe this is the best way in which we can make a significant contribution to the success of the 30-in. chamber operation at NAL. We have experience at Notre Dame with optical and wire chambers and have developed the hardware and software needed to output spark chamber information on magnetic tape. A small computer and a tape unit can be made available. In addition

to physicists, two technicians and an engineer are available for use in this project.

C. Picture Requirements:

We are requesting a total of 200,000 pictures at 150 GeV/c and 100,000 pictures each at 50 GeV/c and 300 GeV/c. (The rationale for choosing these energies is discussed elsewhere in this proposal.) In order to determine the number of pictures required we have assumed a beam intensity of 10 π^- per picture, a constant total cross section (24mb), a fiducial length of 15", and an average charged-track multiplicity which varies as ln(s). We finally assume reasonable longitudinal and transverse momentum distributions based on our experience at lower energy. We show in Table V the results of our calculations.

Table V
Estimate of Measurable Negative Tracks

Beam Momentum (GeV/c)	50	150	300
Pictures Requested	100K	200K	100K
Events	32K	64K	32K
Average Negative Track Multiplicity	2.67	3.31	3.70
Number of Negative Tracks	85.44K	211.84K	118.4K
Negative Tracks for $x < 0$	28.2K	69.8K	39.0K
Measurable Range of x	$-1.0 < x < +0.22$	$-1.0 < x < +0.12$	$-1.0 < x < +0.09$
Measurable Negative Tracks for $x > 0$	38.5K	61.7K	27.8K
Total Measurable Negative Tracks	66.7K	131.5K	66.8K

The last row shows the number of tracks which will be analyzable at each energy. The number at 150 GeV/c is the minimum necessary to study the correlations between x, Q, and n. The numbers at 50 and 300 GeV/c represent the number required to test scaling.

D. Data Analysis.

The Notre Dame group is capable of a fast data reduction on this experiment for two reasons. First, we have done this type of experiment at lower energy and are geared up for doing measuring in an "inclusive" experiment. Second, we have considerable experience with the 30-in. chamber. (We have published four papers based on 30-in. chamber data.) Thus we will be able to analyze the data with no "lead-time" requirement for debugging geometry reconstruction programs.

The measuring system used consists of five measuring machines on-line to a DDP-124 operating 16 hrs./day, 5 days/week. We have measured 120,000 tracks in 25 weeks on a similar experiment at lower energy. (Much of this work was done with only 4 machines, while improved film-transports were being installed.) We are now operating at a rate of 8,000 tracks/week (prescanned film) and quote the previous experiment's rates only as a lower limit to our capability.

The Notre Dame scanning and measuring staff is familiar with the techniques used in measurement of negative tracks for an "inclusive" experiment. The combination of conventional measuring machines and trained operators is highly efficient for the proposed experiment, since

positive tracks can be efficiently discarded without further time and analysis. In cases where the curvature of a track is hard to distinguish, a simple on-line reconstruction can be performed and the results immediately presented to the measurer. For rapid scanning, we are equipped with a system for putting results from scan tables directly on magnetic tape. The information can be immediately supplied to the measurer via the on-line computer. If information about beam tracks were available on magnetic tape, it could be directly integrated into the system.

We plan to concentrate efforts on the analysis of this experiment as soon as the data become available. Checks of the data analysis system will be made in advance. Since our system from measurement to analysis is presently operable, we expect to have preliminary physics results within 10 weeks of the acquisition of data.

E. Resolution.

We show in Fig. 7 the estimated resolution in p_{lab} as a function of p_{lab}. These errors are for flat tracks and use the expression for conventional measuring machines with optimized measurements given by Fischer[17]:

$$\frac{\Delta p}{p} = \left[\frac{3.55\, p^2 \epsilon^2}{H^2 L^2} + \frac{.133\, \alpha}{H^2 L} \right]^{1/2}$$

were p is the momentum in GeV/c, ϵ is the point setting error in microns, L is the length of the track in cm., H is the magnetic field in kilogauss, and $\alpha \equiv \ln(4.8\, p) + \ln(145\, p/mc)$. The curve is calculated for relativistic

pions ($\beta \approx 1$) with p in GeV/c, $\epsilon = 100\mu$, H = 32 kilogauss, and L = 15". (Since the 30-in. chamber may operate initially at a lower value of H, this figure should be scaled accordingly. However the value $\epsilon = 100\mu$ is conservative and 15" is near the minimum track length for forward tracks, so the results of the figure should be qualitatively correct in any case.) Fig. 8 shows how this resolution determines the uncertainty in x for positive x. (All negative values of x yield laboratory momenta which are easily analyzed with good resolution.) From these figures it is clear that positive x can be measured to good accuracy ($\Delta x = 0.01$) out to about 0.22 for 50 GeV/c, to 0.12 for 150 GeV/c, and to 0.09 for 300 GeV/c with the bare bubble chamber. Thus we should be able to determine the value of the slope b in the expression $dN/dx = Ce^{-b|x|}$ for positive x even at these high energies. The value of b for negative x will of course be determined much more accurately and may perhaps be even more relevant to the understanding of the basic physics involved. Fig. 8 might be somewhat optimistic on four grounds. First, H may be less than 32KG initially. Second, the computation is for flat tracks--dipping tracks increase the errors somewhat. Thirdly, the computation is for forward tracks (Q = 0). Actually Δx depends both on x and Q for a given track. And finally, the measuring failure rate will increase significantly at large positive x. We have estimated each of these effects and find that the range of positive x which can be measured may be somewhat smaller than calculated according to Fig. 8. However, we find in any case: that all negative x at all energies is measurable; that the

slope b can be determined for positive x at 50 and 150 GeV/c; and that b can probably be determined for positive x even at 300 GeV/c. The validity of this statement is shown in Fig. 9 where values of x are shown for various values of Q for a track with laboratory momentum of 20 GeV/c ($\frac{\Delta p}{p} \sim 8.2\%$ for a flat track), a reasonable estimate for the highest momentum which can be consistently measured in the 30-in. "bare" bubble chamber. This figure indicates that for Q = .5 GeV/c, we can consistently measure tracks with x = + 0.39 at 50 GeV/c, x = + 0.13 at 150 GeV/c and x = + 0.06 at 300 GeV/c.

The resolution in the transverse momentum Q depends on how well one measures p, the momentum of the secondary track, θ, the laboratory angle of the secondary track, and θ_B, the angle of the beam track. We have estimated the resolution ΔQ as a function of Q for various laboratory momenta as shown in Fig. 10. In this calculation, an uncertainty in the beam angle of 0.4 mrad is assumed -- comparable to the full spread expected for the beam. Again ϵ is taken to be 100μ and the outgoing track is assumed to be flat and 15" in length. These assumptions lead to an uncertainty in secondary track angle of 1.0 mrad for all secondary momenta above about 1 GeV/c. Despite the assumption of flat tracks, the estimates of ΔQ shown here are conservative since ϵ may well be less than 100μ and the average track length greater than 15". Thus the transverse momentum resolution will be adequate for studying the properties of the "inclusive" reactions.

One of the difficulties of this experiment is simply counting the number of outgoing particles. At low energies, this is a very trivial

job, but as s increases, track multiplicity increases and more particles are emitted in a small forward cone. Since the functional dependence of $< n >$ and the distribution of multiplicities are of interest, we would like to determine these quantities accurately. To determine the feasibility of such a measurement, we assume that when two tracks are separated by one full bubble diameter ($\sim 100\mu$ in space), the tracks can be resolved either by eye or with the aid of a microscope. The kinematics, even at 300 GeV/c, show that the probability of two tracks remaining parallel with a separation of less than one bubble diameter for 15'' is very small. Thus we feel that n can be measured, although not without considerable effort, at all energies proposed in this experiment.

REFERENCES

1 R. P. Feynman, "Behavior of Hadron Collisions at Extreme Energies," talk given at the Third International Conference on High Energy Collisions, S.U.N.Y. Stony Brook, September 1969; Phys. Rev. Letters 23, 1415 (1969).

2 J. Benecke, T. T. Chou, C. N. Yang, E. Yen, Phys. Rev. 188, 2159 (1969); T. T. Chou and C. N. Yang, Phys. Rev. Letters 25, 1072 (1970).

3 R. Hagedorn, Supp. Nuovo Cimento III, 147 (1965). A summary of references to the thermodynamic model is given in R. Hagedorn, "Remarks on the Thermodynamic Model of Strong Interactions," CERN Report TH-1174 (1970). See also S. Frautschi, "A Statistical Bootstrap Model of Hadrons" Cal. Inst. of Technology Report CALT-68-286 (1970).

4 D. Amati, A. Stanghellini, and S. Fubini, Nuovo Cimento 26, 896 (1962); L. Caneschi and A. Pignotti, Phys. Rev. Letters 22, 1219 (1969); N. F. Bali, L. S. Brown, R. D. Peccei, and A. Pignotti, Phys. Rev. Letters 25, 557 (1970); Chan Hong-Mo, C. S. Hsue, C. Quigg, and J. M. Wang, Phys. Rev. Letters 26, 672 (1971).

5 Proceedings of the Colloquium on High Multiplicity Hadron Interactions, Ecole Polytechnique, Paris, May 13-15, 1970.

6 V. P. Kenney, invited paper at the Washington APS Meeting, 1971; N. N. Biswas, N. M. Cason, V. P. Kenney, J. T. Powers, W. D. Shephard and D. W. Thomas, Phys. Rev. Letters (to be published).

7 A. Erwin, "Multiparticle Production," Conference on Expectations for Particle Reactions at the New Accelerators, Madison, Wisc., 1970; J. W. Elbert, A. R. Erwin, S. Mikamo, D. Reeder, Y. Y. Chen,

W. D. Walker and A. Weinberg, Phys. Rev. Letters 20, 124 (1968); J. W. Elbert, A. R. Erwin, and W. D. Walker, to be published.

8 W. Ko and R. L. Lander, to be published; R. L. Lander, private communication.

9 D. B. Smith, R. J. Sprafka, and J. A. Anderson, Phys. Rev. Letters 23, 1064 (1969); E. W. Anderson, E. J. Bleser, G. B. Collins, T. Fujii, J. Menes, F. Turkot, R. A. Carrigan, R. M. Edelstein, N. C. Hien, T. J. McMahon, and I. Nadelhaft, Phys. Rev. Letters 19, 198 (1967); D. G. Crabb, J. L. Day, N. P. Johnson, P. Kalbaci, A. D. Krisch, M. T. Lin, M. L. Marshak, J. K. Randolph, P. Schmueser, A. L. Read, K. W. Edwards, J. G. Asbury, G. J. Marmer, and L. G. Ratner, Phys. Rev. D1, 645 (1971). Valuable, if limited, information on pp collisions at cosmic ray energies has been presented by the Echo Lake Collaboration, Phys. Rev. Letters 25, 1679 (1970) and 26, 728 (1971).

10 An alternative definition, $x = 2p_{\parallel}/\sqrt{s}$, is equivalent in the high energy limit and differs only by a scale factor at lower energies.

11 C. E. DeTar, Phys. Rev. D3, 128 (1971).

12 D. Silverman and C. I. Tan, Phys. Rev. D3, 991 (1971).

13 N. F. Bali, A. Pignotti, and D. Steele, Phys. Rev. D3, 1167 (1971).

14 E. Yen and E. L. Berger, Phys. Rev. Letters 24, 695 (1970); E. L. Berger, private communication.

15 J. Lach and S. Pruss, "Hadron Beams in the Neutrino Area," NAL Internal Report TM-285, January 25, 1971.

16 "Extrapolated Ratios of K^- and $\bar{p}$ to π^- from High Energy Protons on Aluminum Measured at Serpukhov," V. E. Barnes, Purdue University High Energy Physics Note #313, April 1, 1971.

17 C. M. Fisher, "Optimization of Bubble Chamber Design Parameters; Measuring Accuracies for Charged Particles," International Colloquium on Bubble Chambers, April, 1967, CERN 67-26 pp.25-47.

FIGURE CAPTIONS

Fig. 1. Distributions of the longitudinal-momentum scaling variable x at 18.5 GeV/c: (a) dN/dx for π^+p data for all-, 4-, 6-, 8-, and 10-prong events; (b) dN/dx for π^-p data for all-, 4-, 6-, 8-, and 10-prong events.

Fig. 2 Distributions of the transverse-momentum-squared, Q^2, for π^+p interactions at 18.5 GeV/c: (a) dN/dQ^2 distributions with $0.0 < x < 0.1$ for all-, 4-, 6-, 8-, and 10-prong events separately; (b) dN/dQ^2 distributions for 4-prong events with $-0.1 < x < 0.0$, $0.0 < x < 0.1$, $0.1 < x < 0.2$, and $0.2 < x < 0.5$.

Fig. 3. Dependence of fitted parameters a and b in 18.5 GeV/c $\pi^{\pm}p$ interactions: (a) a as a function of n, (b) a as a function of x, (c) b as a function of n, and (d) b as a function of Q^2, for all π^+p data. The corresponding parameters for π^-p data are shown in (e) through (h).

Fig. 4. (a) Distribution of $(2E/\pi\sqrt{s})(d\sigma/dx)$ as a function of x for π^- in 18.5 and 8 GeV/c π^-p interactions. (b) Ratio of $(2E/\pi\sqrt{s})(d\sigma/dx)$ at 18.5 and 8 GeV/c as a function of x. (c) Distribution of $d\sigma/dx$ as a function of x in 18.5 and 8 GeV/c π^-p interactions. (d) Ratio of $d\sigma/dx$ at 18.5 and 8 GeV/c as a function of x. The curves shown in (a) and (c) for the two momenta are shifted by a factor of 10. The error bars shown in (b) and (d) indicate typical statistical uncertainties.

Fig. 5. Distributions of the rapidity w in the c.m. system for π^- in π^-p interactions at 18.5 GeV/c for all-, 4-, 6-, and 8-prong events.

Fig. 6. Distributions of dN/dQ for π^- in π^+p interactions at 18.5 GeV/c for events with $0.00 < x < 0.04$, $0.04 < x < 0.10$, $0.10 < x < 0.20$, and $0.20 < x < 0.50$. The curves are described in the text.

Fig. 7. Momentum resolution, $(\Delta p/p)$, for relativistic tracks in the 30-in. hydrogen bubble chamber. Calculations are described in the text.

Fig. 8. Resolution in x for $x > 0$ estimated for π^- mesons in the 30-in. bubble chamber. Solid curves are shown for π^-p interactions at incident momenta of 50, 150, and 300 GeV/c. The dotted lines correspond to specific longitudinal momenta in the laboratory.

Fig. 9. Values of the scaling variable x as a function of transverse momenta Q for π^- mesons with a laboratory momentum of 20 GeV/c. Curves are shown for π^-p interactions at incident momenta of 50, 150, and 300 GeV/c.

Fig.10. Resolution in transverse momentum Q as a function of Q for relativistic tracks in the 30-in. hydrogen bubble chamber. Curves are shown for laboratory momenta of 5, 10, 15 and 20 GeV/c. Calculations are described in the text.

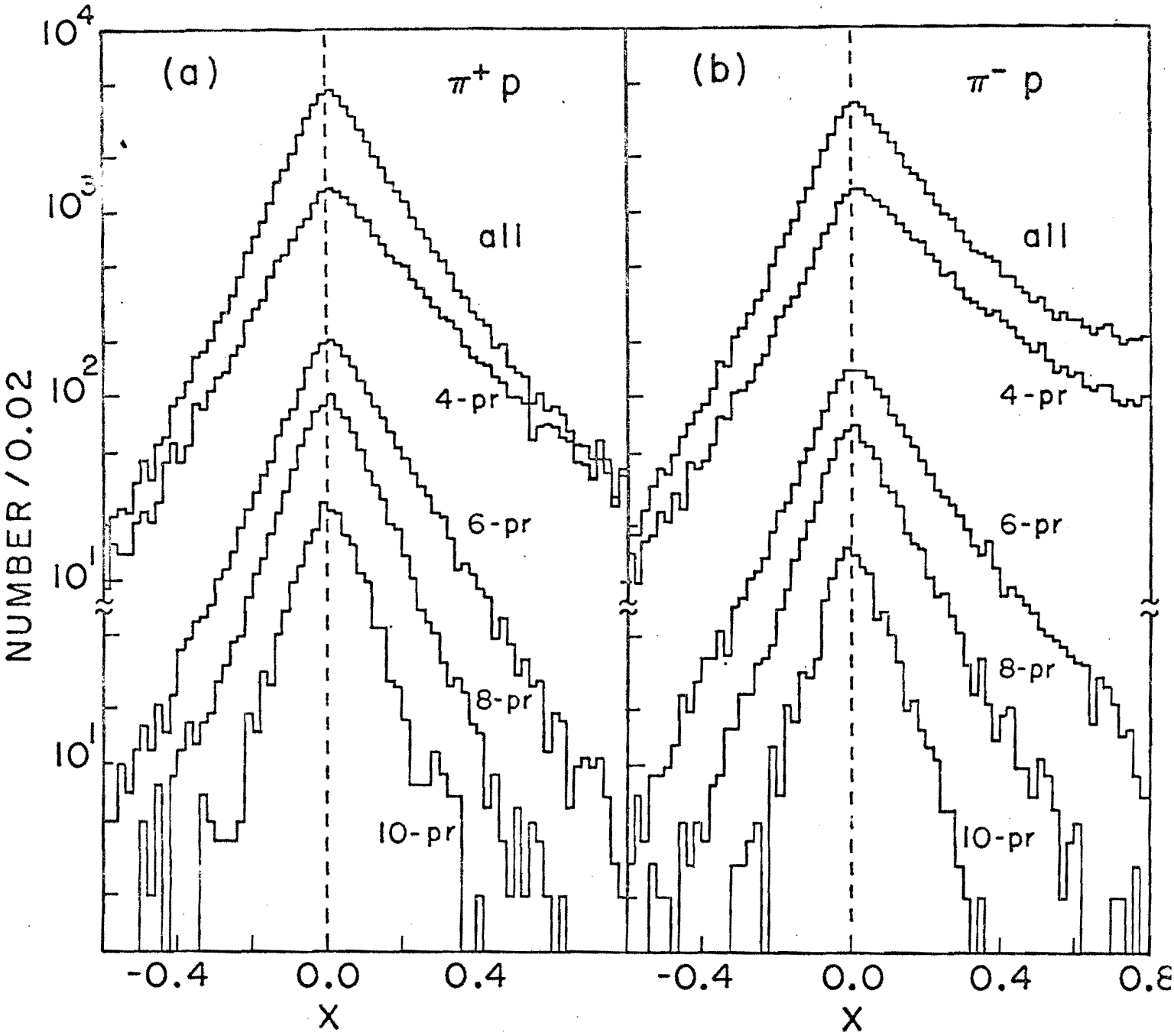
(a)
$\pi^+ p$
(b)
$\pi^- p$
all
4-pr
6-pr
8-pr
10-pr
NUMBER / 0.02
10^4
10^3
10^2
10^1
10^1
-0.4
0.0
0.4
0.8
X

Fig. 1

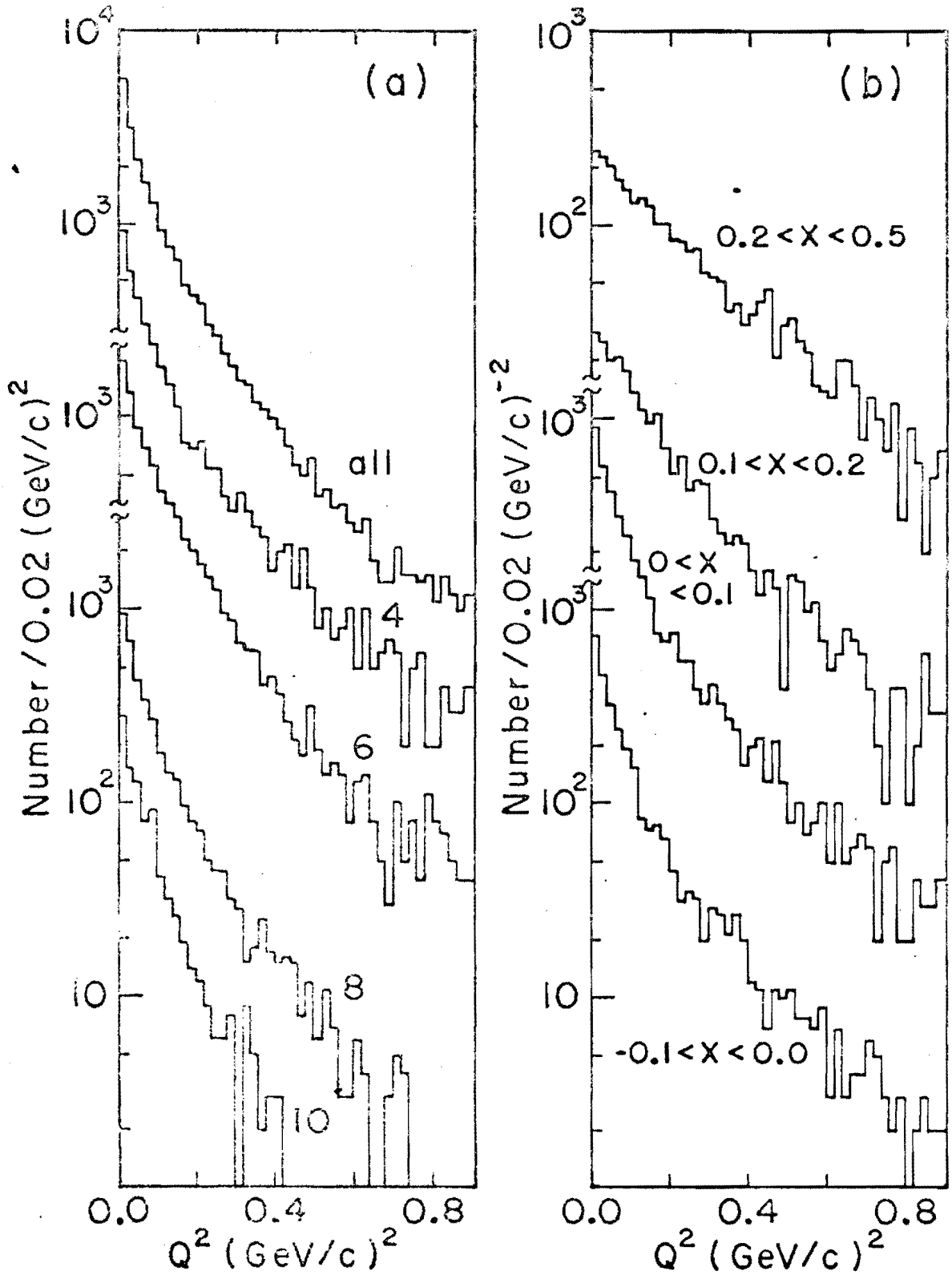
(a)
(b)
all
4
6
8
10
0.2<X<0.5
0.1<X<0.2
0<X<0.1
-0.1<X<0.0
Number /0.02 (GeV/c)^2
Number /0.02 (GeV/c)$^{-2}$
Q^2 (GeV/c)^2
Q^2 (GeV/c)^2
0.0
0.4
0.8
10
10^2
10^3
10^4

Fig. 2

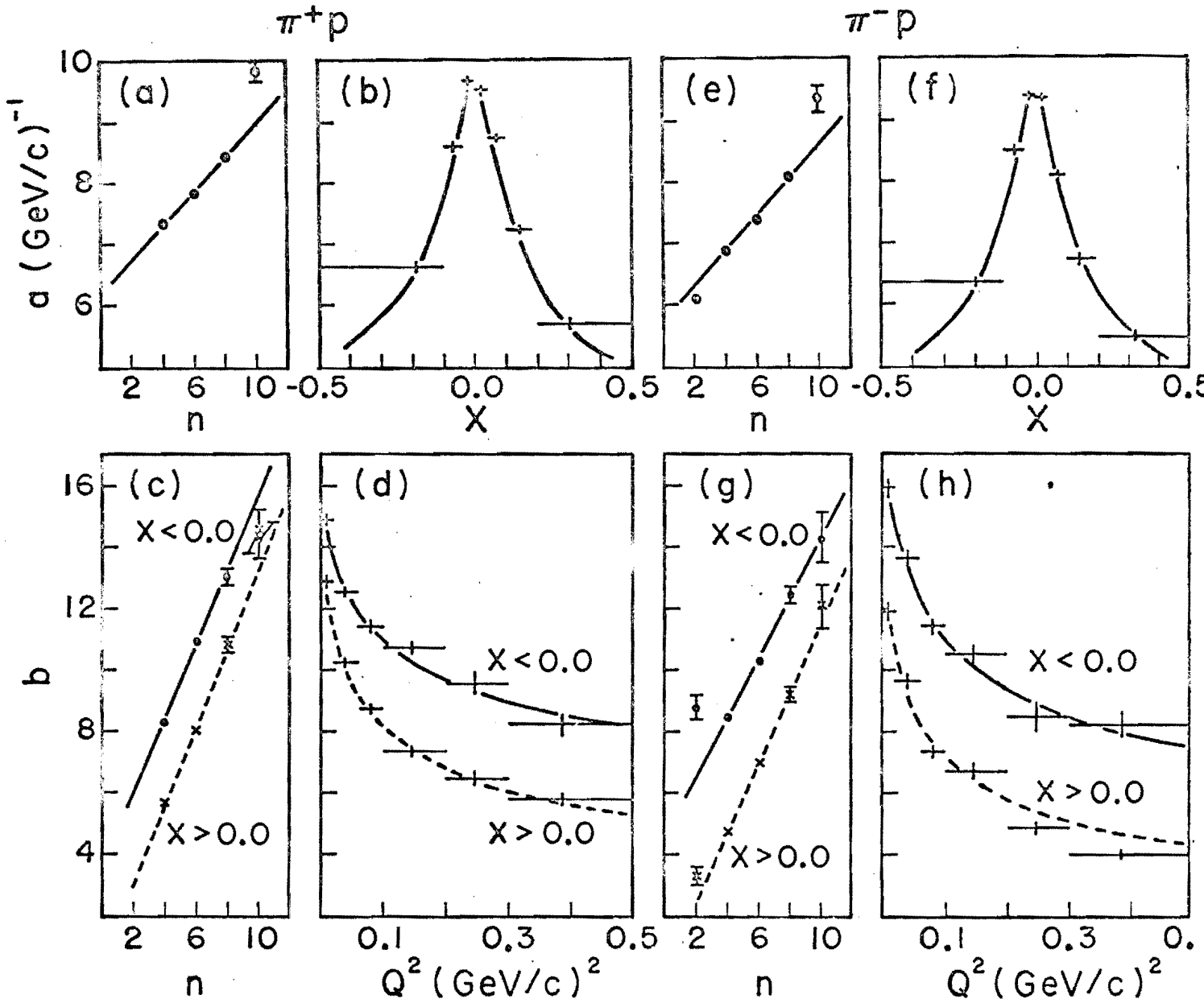
π⁺p
π⁻p
(a)
(b)
(e)
(f)
a (GeV/c)⁻¹
10
8
6
2
6
10
n
-0.5
0.0
0.5
X
(c)
(d)
(g)
(h)
b
16
12
8
4
X<0.0
X>0.0
0.1
0.3
0.5
Q² (GeV/c)²

Fig. 3

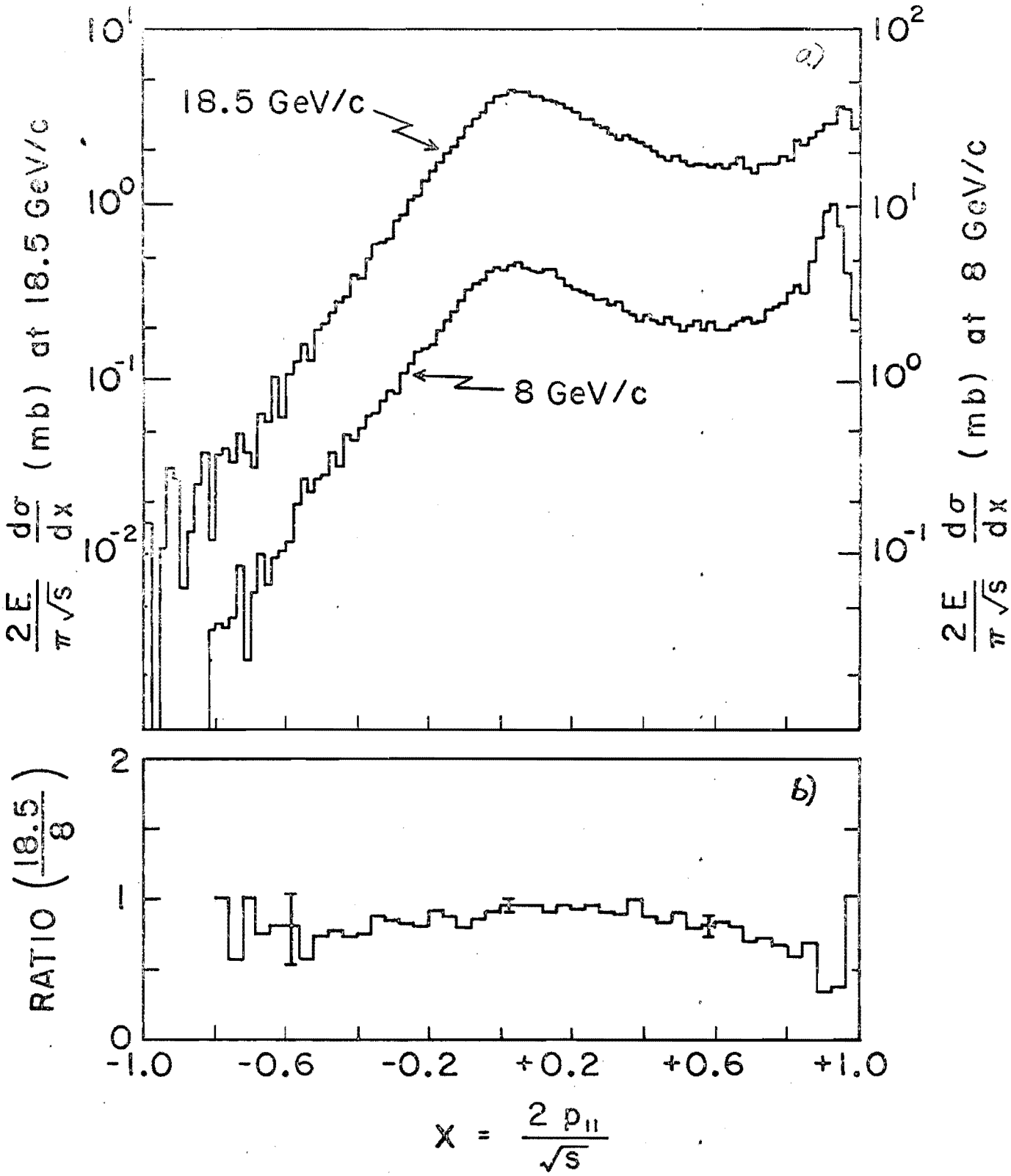
a)
18.5 GeV/c
8 GeV/c
$\frac{2E}{\pi\sqrt{s}}\frac{d\sigma}{dx}$ (mb) at 18.5 GeV/c
$\frac{2E}{\pi\sqrt{s}}\frac{d\sigma}{dx}$ (mb) at 8 GeV/c
b)
RATIO $\left(\frac{18.5}{8}\right)$
$x = \frac{2\,p_{\parallel}}{\sqrt{s}}$

Fig. 4

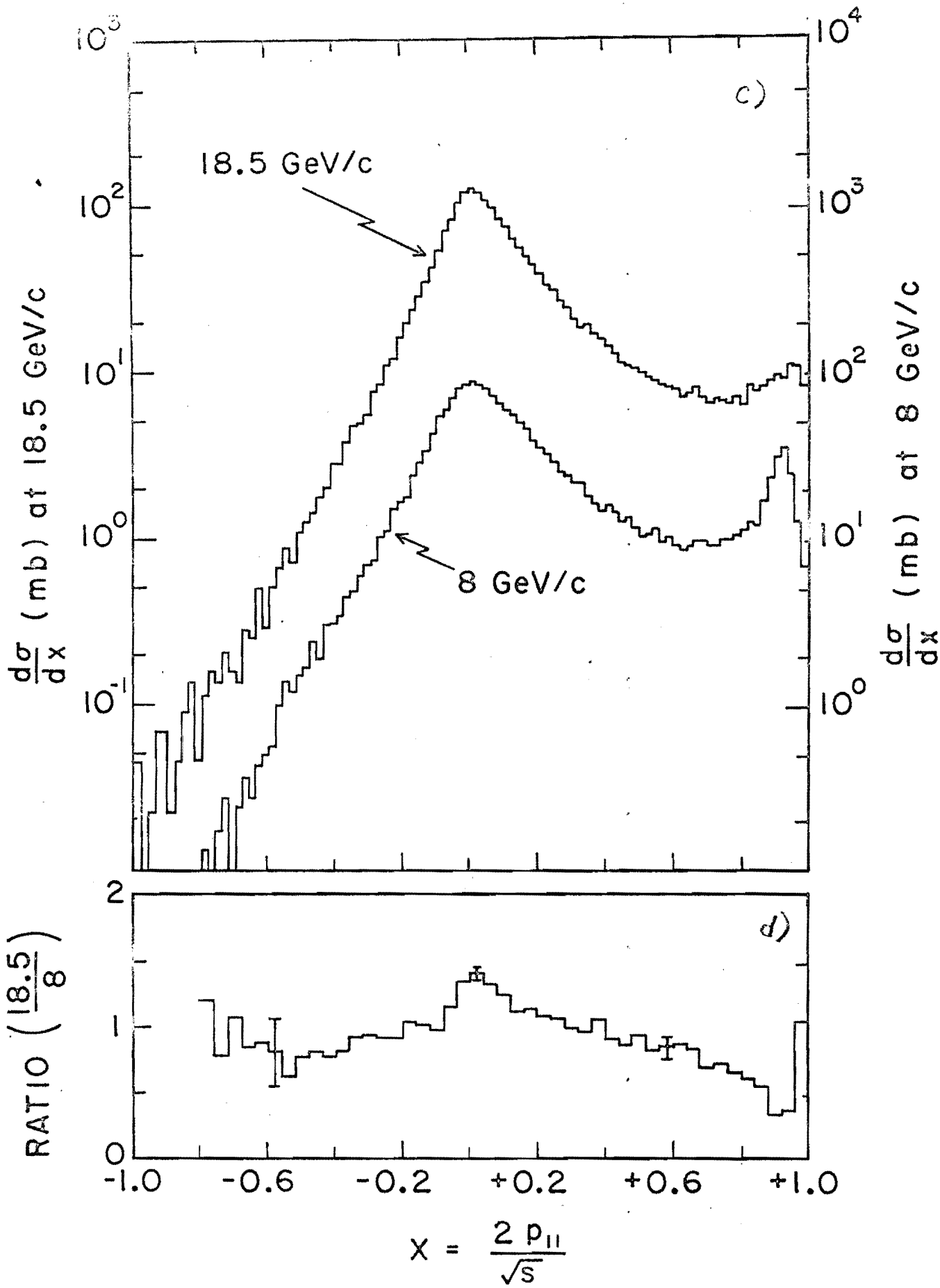
c)
18.5 GeV/c
8 GeV/c
$\frac{d\sigma}{dx}$ (mb) at 18.5 GeV/c
$\frac{d\sigma}{dx}$ (mb) at 8 GeV/c
d)
RATIO $\left(\frac{18.5}{8}\right)$
$X = \frac{2\,p_{\parallel}}{\sqrt{s}}$

Fig. 4

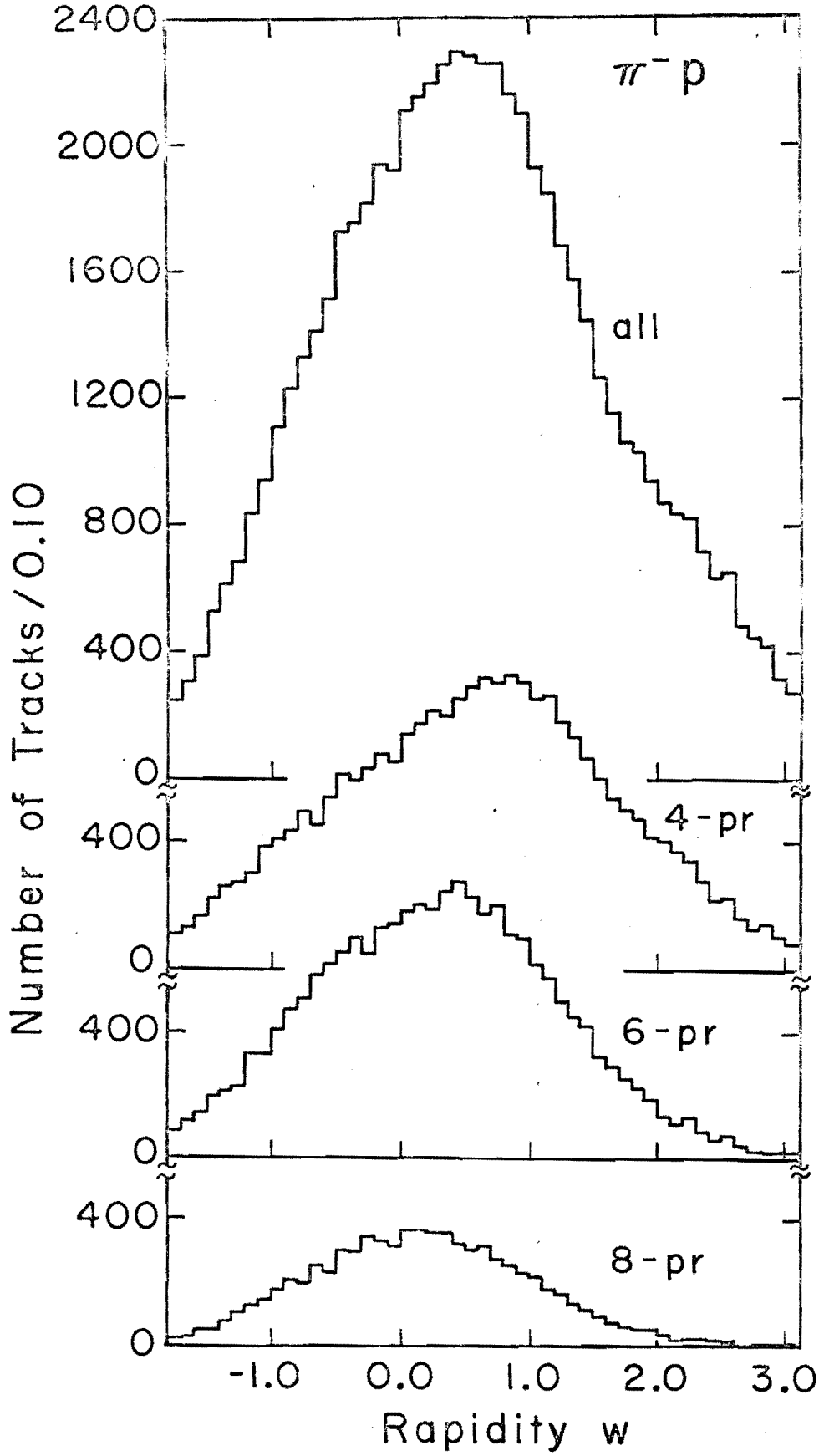
2400
2000
1600
1200
800
400
0
400
0
400
0
400
0
$\pi^- p$
all
4-pr
6-pr
8-pr
Number of Tracks/0.10
-1.0
0.0
1.0
2.0
3.0
Rapidity w

Fig. 5

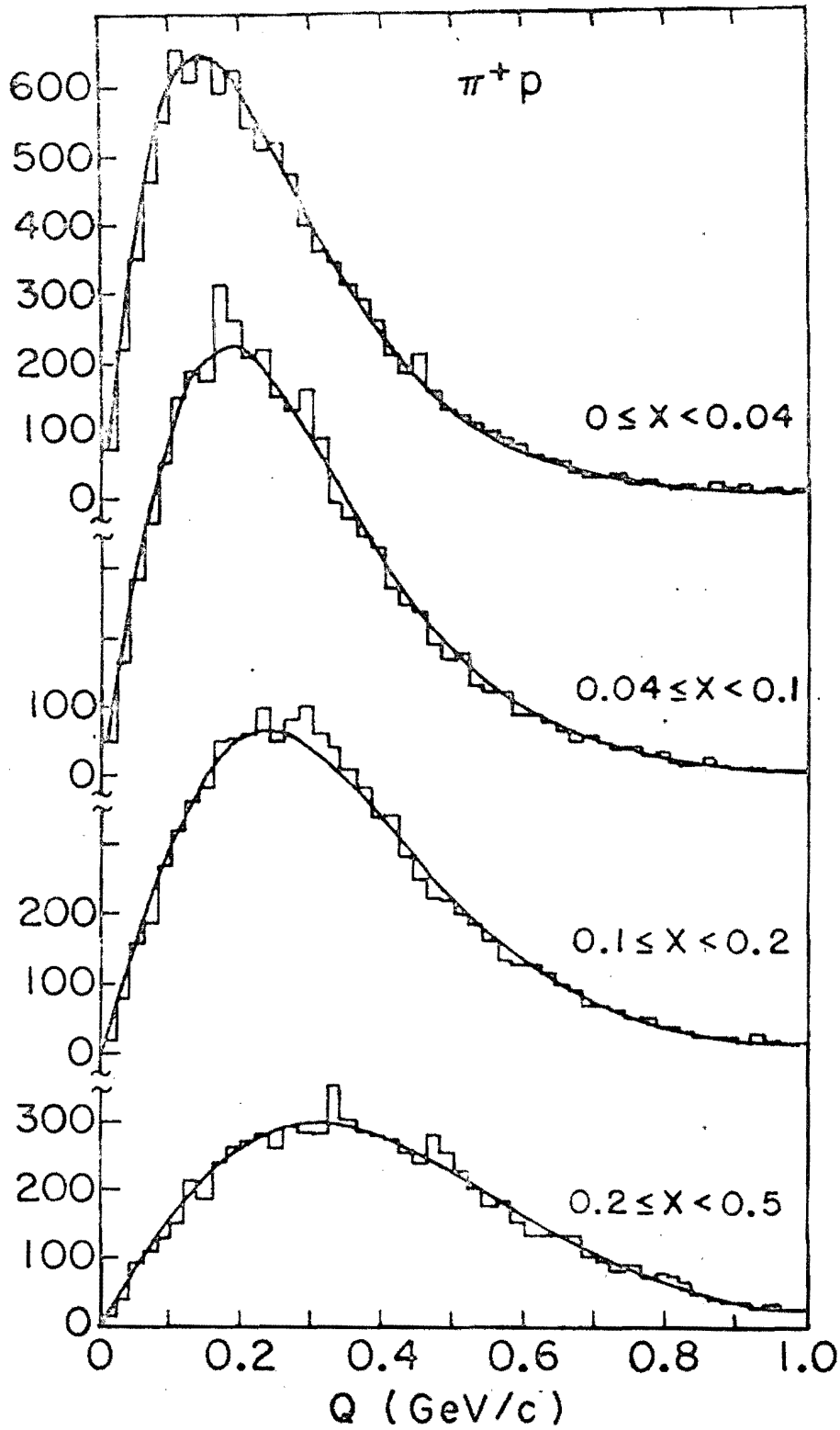
$\pi^+ p$
600
500
400
300
200
100
0
$0 \le X < 0.04$
100
0
$0.04 \le X < 0.1$
200
100
0
$0.1 \le X < 0.2$
300
200
100
0
$0.2 \le X < 0.5$
0
0.2
0.4
0.6
0.8
1.0
Q (GeV/c)

Fig. 6

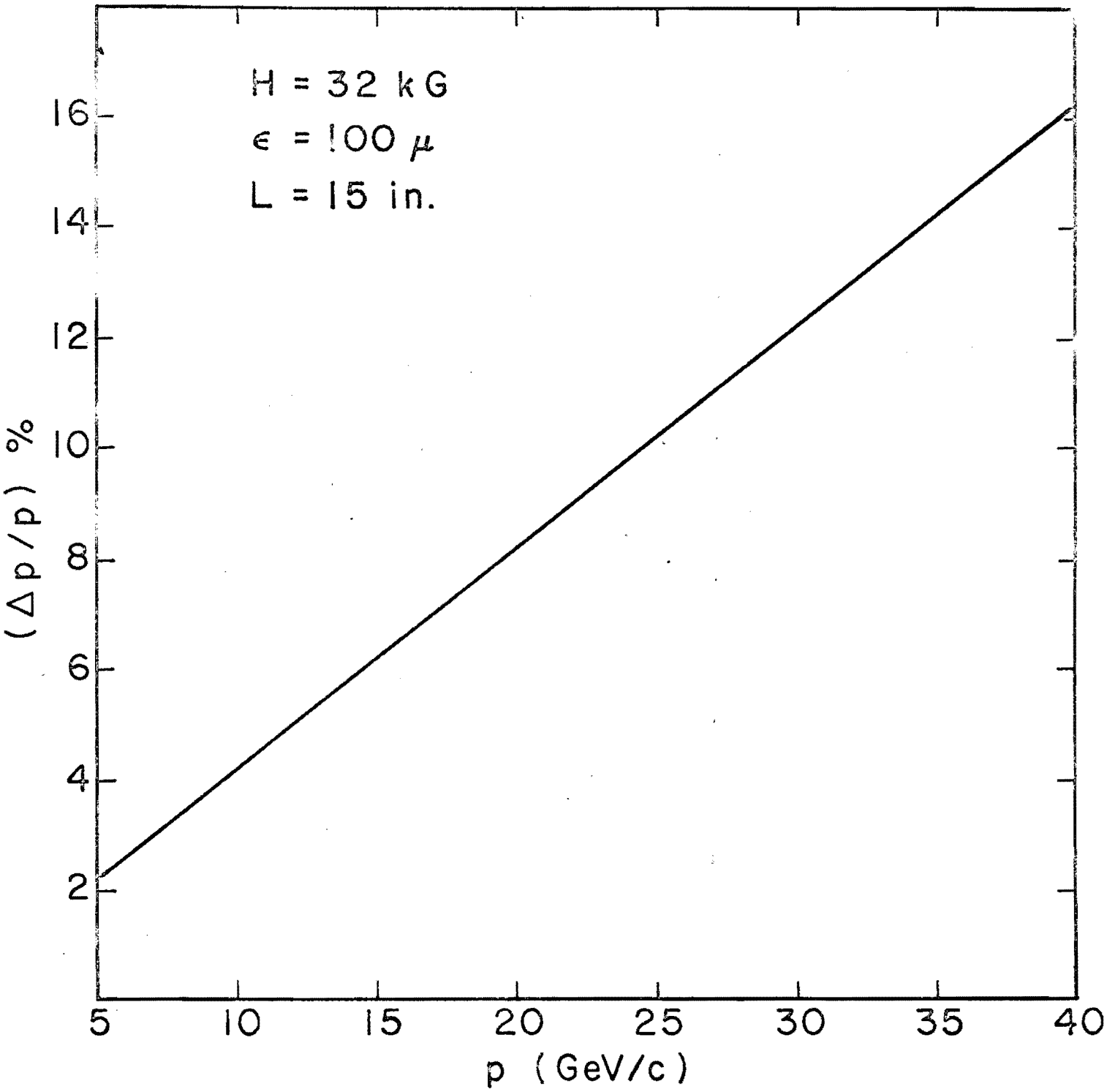
H = 32 kG
ϵ = 100 μ
L = 15 in.
16
14
12
10
8
6
4
2
(Δp/p) %
5
10
15
20
25
30
35
40
p (GeV/c)

Fig. 7

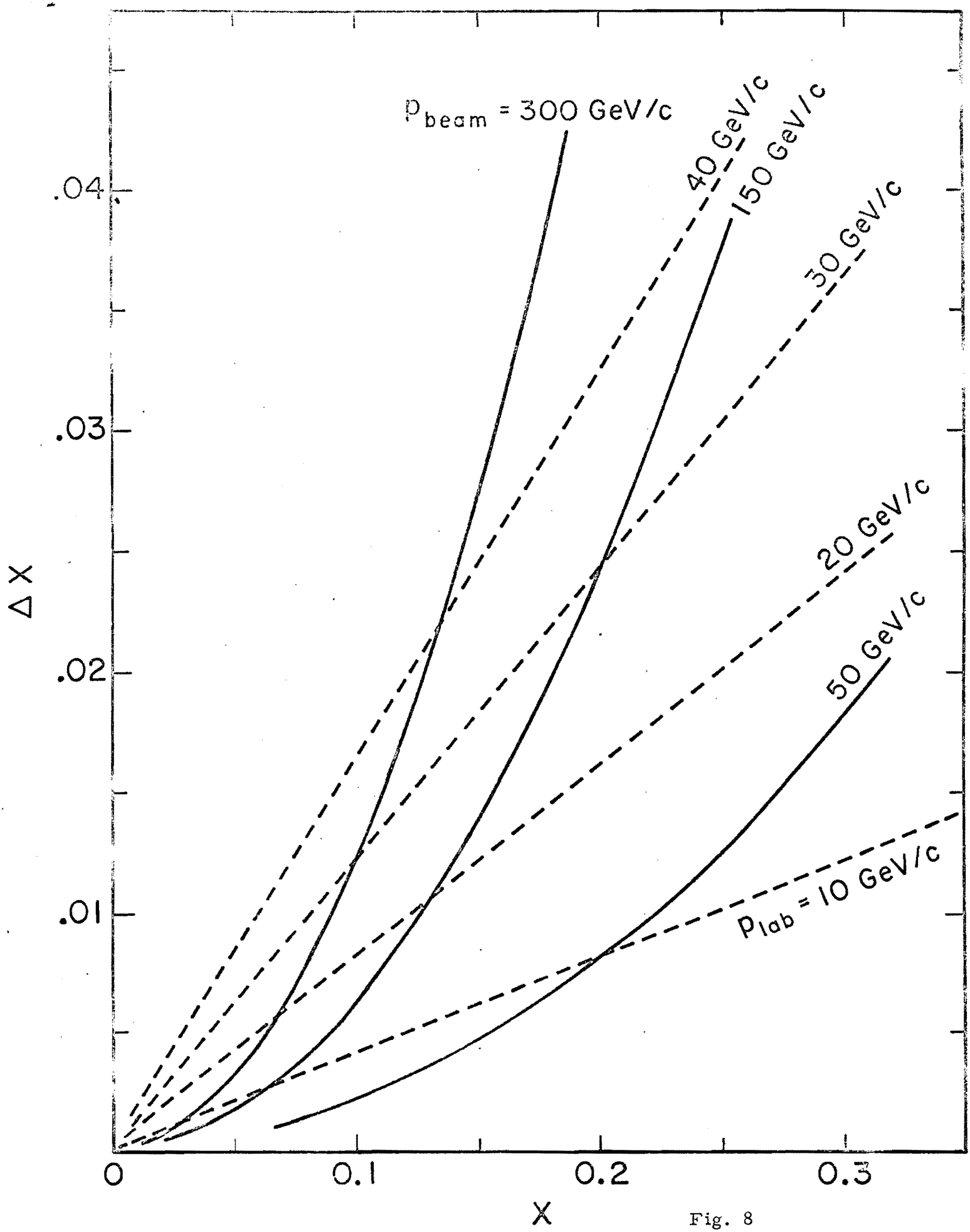
p_{beam} = 300 GeV/c
40 GeV/c
150 GeV/c
30 GeV/c
20 GeV/c
50 GeV/c
p_{lab} = 10 GeV/c
.04
.03
.02
.01
ΔX
0
0.1
0.2
0.3
X

Fig. 8

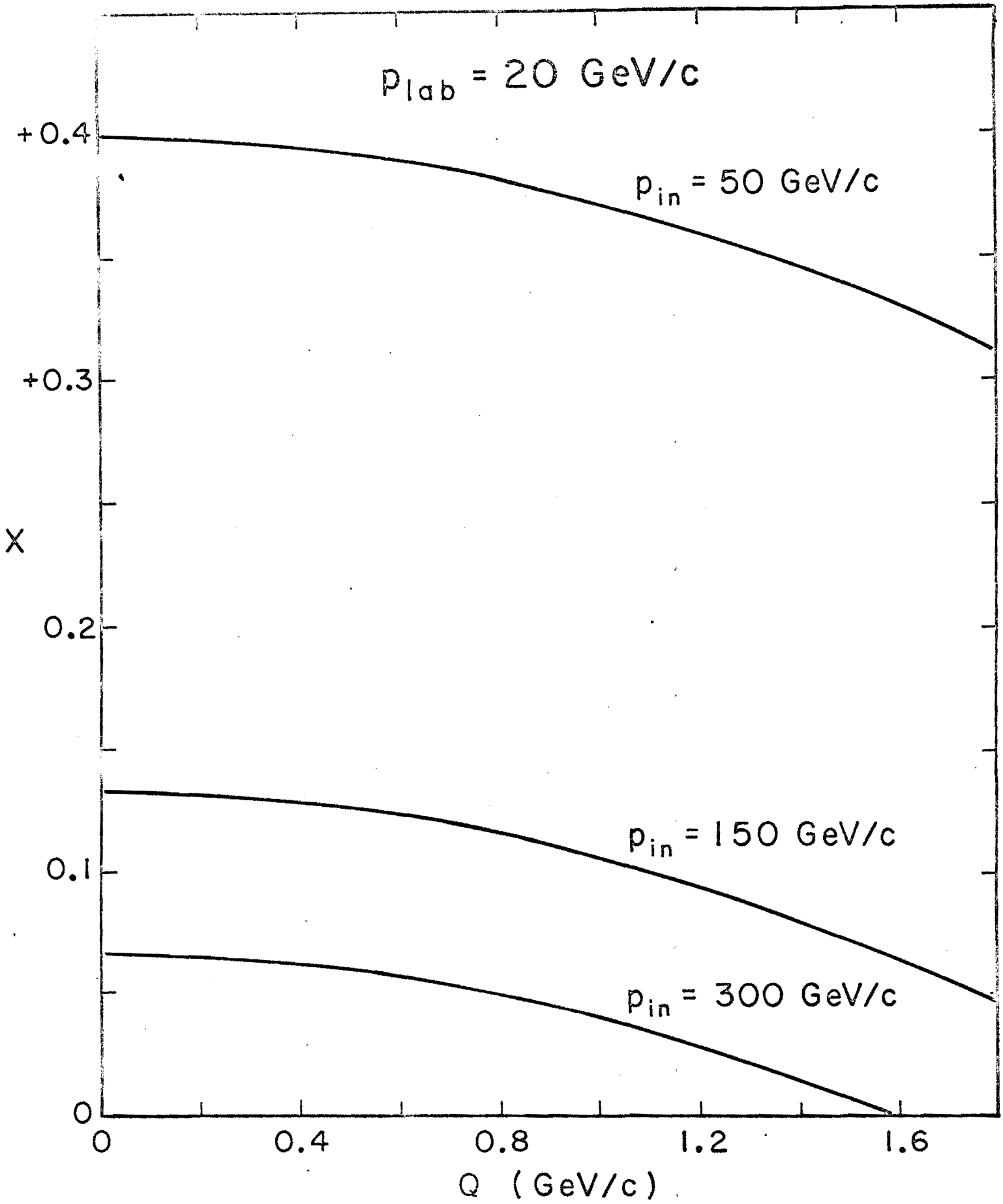
p_{lab} = 20 GeV/c
+0.4
+0.3
0.2
0.1
0
X
p_{in} = 50 GeV/c
p_{in} = 150 GeV/c
p_{in} = 300 GeV/c
0
0.4
0.8
1.2
1.6
Q (GeV/c)

Fig. 9

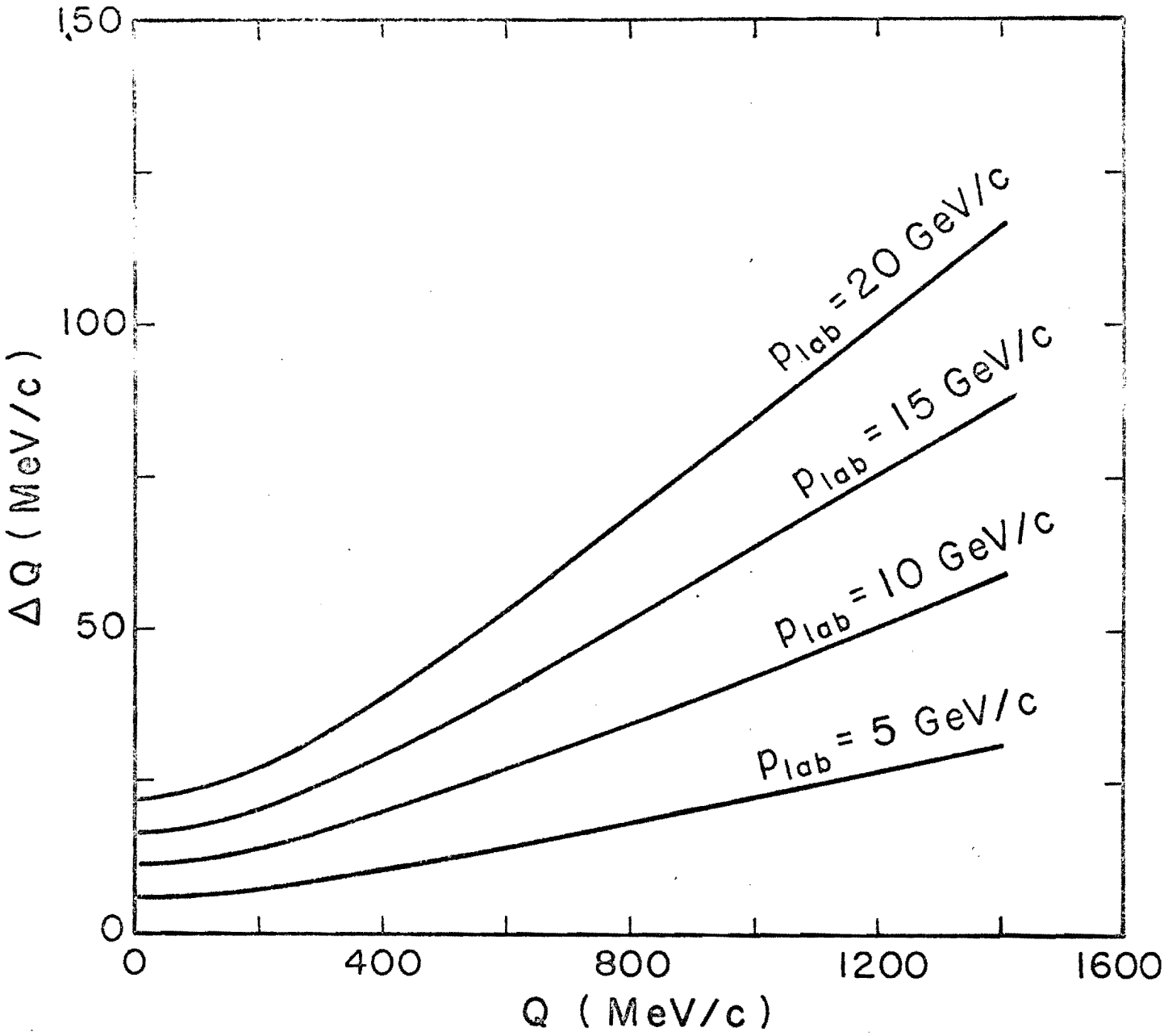
150
100
50
0
ΔQ (MeV/c)
0
400
800
1200
1600
Q (MeV/c)
p_{lab} = 20 GeV/c
p_{lab} = 15 GeV/c
p_{lab} = 10 GeV/c
p_{lab} = 5 GeV/c

Fig. 10